Origin and modulation of the narrowband gamma oscillation in the mouse visual system

Aman B Saleem[1,2,3], Anthony D Lien[4], Michael Krumin[1,2,3], Bilal Haider[1,A], Miroslav Román Rosón[5,6], Aslı Ayaz[1,B], Kimberly Reinhold[4], Laura Busse[5,C], Matteo Carandini[1,7] & Kenneth D Harris[2,3,7]

[1]UCL Institute of Ophthalmology, [2]UCL Institute of Neurology, [3]UCL Department of Neuroscience, Physiology, and Pharmacology, University College London, UK, [4]Division of Biological Sciences, University of San Diego, USA, [5]Weiner Reichardt Centre for Integrative Neuroscience, [6]Graduate Training Centre of Neuroscience, University of Tübingen, Germany, [7]Co-senior author.

Present addresses: [A]Coulter Dept. of Biomedical Engineering, Georgia Institute of Technology & Emory University, USA; [B]Brain Research Institute, University of Zurich, Switzerland; [C]Division of Neurobiology, Department Biology II, LMU Munich, Germany

Summary

Visual cortex (V1) exhibits two types of gamma oscillation: a well-characterized broadband (30-90Hz) rhythm, and a narrowband oscillation occurring at frequencies close to 60 Hz in mice. We investigated the source of narrowband gamma, the factors modulating its strength, and its relationship to broadband gamma. Narrowband and broadband gamma power were uncorrelated. Increasing visual contrast had opposite effects on the two kinds of gamma activity: it increased broadband power, but suppressed the narrowband oscillation. Narrowband power was strongest in layer 4, and was mediated primarily by excitatory currents entrained by rhythmically firing neuronal ensembles in the lateral geniculate nucleus (LGN). Silencing the cortex optogenetically did not affect narrowband rhythmicity in either LGN spike trains or cortical EPSCs, suggesting that this oscillation reflects unidirectional flow of information from LGN to V1.

Highlights

- Local field potential in mouse primary visual cortex exhibits a pronounced narrowband gamma oscillation close to 60 Hz.
- Unlike broadband gamma, narrowband gamma is present in excitatory synaptic inputs to individual V1 neurons, and suppressed by visual contrast
- Narrowband gamma is highest in the thalamorecipient layer 4
- Lateral geniculate nucleus neurons fire synchronously at the narrowband gamma frequency, independent of V1 activity.

Introduction

High frequency gamma oscillations are produced by a wide range of brain circuits and are thought to reflect multiple phenomena. Oscillations in a broad gamma range (30-90 Hz) have long been observed in regions including isocortex (Engel et al.,2001; Fries,2009), hippocampus (Bragin et al.,1995), amygdala, striatum (Popescu et al.,2009), and cerebellum (Middleton et al.,2008). In cortex, these oscillations are believed to arise from the precisely-timed synchronization of inhibitory networks (Cardin et al.,2009; Penttonen et al.,1998; Sohal et al.,2009; Wang and Buzsaki,1996), and

have been implicated in a wide range of functions including coherent transmission of information between neuronal assemblies (Fries,2005, 2009), multiplexing of information (Lisman and Idiart,1995), or binding of multiple features of a sensory scene(Singer). Recently, however, it has become clear that the gamma oscillation in fact reflects multiple phenomena, and that a single neuronal circuit can support multiple types of gamma oscillation. In hippocampal area CA1, for example, gamma oscillations occurring in two distinct frequency bands are coherent with two distinct input sources (Colgin et al.,2009), and have been proposed to provide separated routes for information from those structures. Understanding the origin of multiple patterns of high-frequency oscillations is essential for understanding the functional roles these oscillations might play.

In the visual cortex, there is evidence for two fundamentally different types of gamma-range oscillation, one with power distributed in a broad band between 30 and 90 Hz, and one that oscillates in a much narrower band. The broadband gamma oscillations have long been described in multiple species including cats (Eckhorn et al.,1988; Gray and Singer,1989), primates (Fries et al.,2001; Kreiter and Singer,1992; Pesaran et al.,2002), rodents (Cardin et al.,2009; Sohal et al.,2009), and humans (Tallon et al.,1995). They are modulated by factors such as stimulus position, context, or cognitive state (Chalk et al.,2010; Fries et al.,2001; Gieselmann and Thiele,2008; Gray and Singer,1989; Pesaran et al.,2002). A fundamentally different gamma oscillation has been reported in visual cortex of anesthetized cats. This oscillation is extremely narrowly-tuned in single experiments, and occurs prominently also in the lateral geniculate nucleus and retina (Koepsell et al.,2010; Neuenschwander and Singer,1996). A gamma oscillation with a sharp band close to 60 Hz, whose power grows with locomotion, has also been observed in primary visual cortex (V1) of awake mice (Lee et al.,2014; Niell and Stryker,2010). The origin of this oscillation, and the behavioral and sensory factors modulating it, are unknown.

Here we investigate the narrowband gamma oscillation in awake mouse V1, and establish its source, the factors that determine its strength and frequency, and its relationship to broadband gamma activity. We find that this oscillation has different properties to the broadband gamma oscillation: its amplitude increases with mean light intensity and with locomotion, but it decreases with visual contrast. The narrowband oscillation occurs independently of broadband gamma activity, indicating that it arises from different mechanisms. These mechanisms involve synaptic excitation more than inhibition, and originate before the visual signals reach the cortex. Indeed, they are present earlier in the visual system, arising at least as early as the lateral geniculate nucleus.

Results

We start by characterizing the narrowband gamma oscillation in mouse primary visual cortex (V1), and how this oscillation depends on mean light intensity. We then explore the synaptic basis of this oscillation, and the way the oscillation is affected by visual contrast and by locomotion. We then turn to the lateral geniculate nucleus (LGN), and to manipulations that establish the source of the narrowband oscillation in the early visual system.

Narrowband gamma in V1

Consistent with previous reports (Lee et al.,2014; Niell and Stryker,2010), when we recorded in V1 of awake mice using multi-electrode arrays (Ayaz et al.,2013; Saleem et al.,2013) we observed a sharp peak in the local field potential (LFP) power spectrum close to 60 Hz (Figure 1A,B; Supplementary Figure 1). The precise frequency of this oscillation was at 61 Hz in this example experiment (Figure

1A-B), and could vary between 55 and 70 Hz in other experiments, with a remarkably narrow bandwidth of 2-5 Hz (Figure 1). These oscillations could not have reflected mains interference, as these recordings were conducted in Europe where (unlike in the United States), the electricity alternates at 50 Hz.

This narrowband oscillation was prominent when the mice viewed a uniform gray screen, but it disappeared when we repeated the experiments in complete darkness (Figure 1A,B). This effect was due to the overall amount of light, not to entrainment of the visual system to the monitor refresh frequency (which can weakly entrain visual cortical neurons (Veit et al.,2011; Williams et al.,2004)). We confirmed this with control experiments where we illuminated the visual field of the mouse not by a monitor, but by a light emitting diode (LED, 570 nm) generating light steadily with direct current (DC) input, or flickering at different rates. We saw a narrowband oscillation close to 60 Hz in all cases, independent of visual flicker rates (Figure 1C; $p>0.1$ t-test for all pairs of stimuli: we compared the peak frequency calculated between different 20% subsets of the recordings).

Unlike broadband gamma oscillations, which involve inhibitory currents (Cardin et al.,2009; Hasenstaub et al.,2005; Sohal et al.,2009), the narrowband gamma oscillation was primarily mediated by excitatory synaptic currents (Figure 1D). To uncover the synaptic basis of the narrowband oscillation, we analyzed intracellular recordings from layer 2/3 regular-spiking (putative pyramidal) neurons in V1 of awake head-restrained mice viewing a uniform gray screen(Haider et al.,2013) (Figure 1D). Excitatory synaptic currents (EPSCs), isolated by voltage clamping the membrane potential near the reversal potential for inhibition, showed a clear peak around 60 Hz similar to that seen in the extracellular LFP. The power in the narrowband gamma frequency range was significantly greater than a baseline prediction based on a smooth power spectrum that excludes this range (the "residual spectrum"; Supplementary Figure S1; $p=0.027$; t-test over $n=11$ recordings). However, we did not observe a similar peak in narrowband gamma power in the inhibitory synaptic currents (IPSCs) recorded from the same neurons during the same stimulus conditions ($p=0.11$; $n = 11$ recordings). This suggests that at least in superficial visual cortex, narrowband gamma is primarily mediated by excitatory synaptic currents.

Narrowband gamma is suppressed by visual contrast

Another fundamental difference between the narrowband gamma oscillation and the broadband gamma activity is that the oscillation decreased with visual contrast (Figure 2A-D). Power in broadband gamma frequencies in V1 has been shown to increase with visual contrasts in multiple species including cats (Eckhorn et al.,1988; Gray and Singer,1989) and primates (Fries et al.,2001; Kreiter and Singer,1992), and humans (Tallon et al.,1995). We measured the spectral power of the primary visual cortical responses to drifting gratings (60^{o} diameter, 2 cycles/sec, 0.05 cycles/°) at different levels of visual contrast. Consistent with previous reports in other species, we found increases in broadband power with increases in contrast in mouse V1 (Correlation $\rho = 0.59 \pm 0.18$, $n = 7$ recordings; Figure 2A-D). Surprisingly, however, we found that narrowband gamma power was instead suppressed by an increase in contrast (Correlation $\rho = -0.43 \pm 0.16$, $n = 7$ recordings; Figure 2C,D).

Narrowband gamma power was suppressed by contrast not only during passive visual presentation, but also while mice used visual inputs to guide locomotion (Figure 2E,F). We recorded V1 activity while mice navigated in a virtual reality environment where visual cues indicated a position that

mice must reach to receive a water reward. The narrowband gamma oscillation increased prominently during inter-trial periods, when the screen was uniform gray (Figure 2E; the increase in narrowband power prior to the onset of the inter-trail interval likely reflects the uniform gray texture of the wall at the far of the virtual corridor). Further, throughout the experiment, the power of this narrowband gamma oscillation was independent of power in broadband gamma range (Figure 2F).

Narrowband gamma is increased in active animals

The strength of narrowband gamma oscillations was related not only to visual factors (presence of light, absence of contrast) but also to the behavioral state of the animal. Consistent with previous reports (Lee et al.,2014; Niell and Stryker,2010), we found that narrowband gamma power is highly correlated with running speed (correlation $\rho = 0.49 \pm 0.04$, mean ± s.e.m, n = 10 recordings). Since the mouse pupil dilates during locomotion (Erisken et al.,2014; McGinley et al.,2015a; McGinley et al.,2015b; Reimer et al.,2014; Vinck et al.,2015), we next confirmed that the effect of locomotion on narrowband gamma power was present even in the absence of pupil dilation. To assess this, we measured gamma power after applying the anti-muscarinic agent Tropicamide to the eye surface. This procedure caused full dilation of the pupil (Supplementary Figure S2A), thus removing the correlation of pupil diameter with running speed. We found that the correlation of narrowband gamma power with running speed persisted even in these conditions of fixed pupil diameter (Correlation $\rho = 0.35$, $p<0.01$, Supplementary Figure 2B).

Narrowband gamma in the early visual system

The power of the narrowband gamma oscillation varied strongly across the depth of visual cortex, and was markedly higher in layer 4 (L4, Figure 3A,B). We recorded the activity across different laminae of V1 using a linear multi-electrode array (16 sites, 50 µm spacing; Figure 3A), and identified layer 4 in each recording as the location showing the earliest current sink (Mitzdorf,1985) in response to a contrast-reversing checkerboard stimulus (Figure 3A). This layer also showed the strongest ~60 Hz narrowband gamma peak during gray screen presentation (Figure 3B). The highest residual power was observed at the same depth as the largest current sink in the recordings (correlation $\rho = 0.98$; $p < 10^{-3}$; n = 6 recordings).

Because layer 4 receives strong inputs from the lateral geniculate nucleus (LGN), we next asked if the gamma oscillation was also present in these inputs, and we found that it is evident in many LGN neurons (Figure 3C-D). We used silicon probes to record from 323 LGN neurons from 7 awake head-fixed mice viewing a uniform gray screen. Inspection of spike-train power spectra revealed that many neurons fired rhythmically, at frequencies close to 60 Hz (Figure 3C-D). We quantified the rhythmicity of each neuron as the power in the narrowband gamma frequency range, compared to a baseline prediction based on a smooth power spectrum (the "residual spectrum"; Supplementary Figure 1). This measure yielded a variety of values across the LGN population (Figure 3D), with 14% of neurons (44/323; n = 18 recordings from 7 animals) showing a narrowband gamma peak greater than 20% of the baseline prediction (dotted line in Figure 3D).

The narrowband gamma oscillation entrained the activity of LGN neurons in a coherent fashion (Figure 3E-H). The narrowband oscillation was also visible in the spike time autocorrelations (Figure 3E), and was coherent between simultaneously recorded pairs of neurons (0.33 ± 0.04; mean ± s.t.d, n = 215 cell pairs where both cells had over 20% residual power), being clearly visible in both the

cross-correlogram and coherence spectrum computed from the spike trains of simultaneously recorded pairs (Figure 3F,G). This coherence indicates that the narrowband gamma oscillation jointly entrains the LGN population. Individual LGN neurons had characteristic phases with respect to the oscillation: computing each neuron's preferred phase in two halves of the data yielded a consistent estimate (correlation $\rho = 0.69$; $p < 10^{-6}$; Figure 3H), and while these phases showed a clear peak near the population mean, a wide range of phases was observed (1.6 ± 40^{o} circular mean and variance of mean phases; Figure 3H). The rhythmicity or phase of gamma entrainment in LGN neurons, moreover, bore no obvious relationship to their visual preferences, such as on-off receptive fields and contrast tuning responses (not shown).

Narrowband gamma in the LGN is independent of V1

The presence of the narrowband gamma oscillation in LGN suggests but does not prove that the cortex inherits this rhythm from thalamus. Indeed, this oscillation could be generated in V1 independent of LGN activity. To investigate this question, we recorded activity in V1 using extracellular multielectrode arrays, while silencing the activity in the LGN by optogenetically activating thalamic reticular nucleus (TRN) neurons(Reinhold et al.,2015). Silencing LGN strongly suppressed LFP activity in V1 at all frequencies, including the narrowband gamma peaks close to 60 Hz (Supplementary Figure 3). This result strongly suggests that the narrowband gamma oscillation measured in V1 is inherited from thalamus.

An alternate hypothesis is that the oscillation could rely on the presence of cortico-thalamic connections. To test this hypothesis, we asked whether silencing V1 would suppress the narrowband gamma oscillation in LGN, and in the excitatory currents to layer 4 cortical neurons. We performed these experiments in VGAT-ChR2 mice, where V1 activity could be silenced optogenetically (Lien and Scanziani,2013). The mice were lightly anesthetized, to facilitate our combined intracellular and extracellular recordings (Figure 4A). This light anesthesia did not affect the presence of the narrowband gamma oscillation: LGN neurons showed rhythmic firing at frequencies close to 60 Hz, and EPSCs recorded simultaneously in layer 4 neurons showed a coherent 60 Hz oscillation (Figure 4B,E).

Silencing the cortex optogenetically did not affect the rhythmicity visible in LGN spike trains and LGN-triggered EPSCs in L4 neurons of V1 (Figure 4B-G). The narrowband peak frequency and power were highly correlated with or without cortical silencing (peak frequency correlation $\rho = 0.91$, $p < 10^{-4}$ and peak power correlation $\rho = 0.85$, $p < 10^{-3}$, $n = 14$ neurons in V1; peak frequency correlation $\rho = 0.88$, $p < 10^{-6}$ and peak power correlation $\rho = 0.57$, $p = 0.0092$, $n = 27$ neurons in LGN with greater than 50% residual power in both conditions; Figure 4D,G). These results demonstrate that the narrowband gamma oscillation in LGN is independent of feedback from V1.

Discussion

In this study we characterized the origin and modulation of the narrowband gamma oscillation in mouse V1. Our measurements indicated several notable differences between this novel narrowband oscillation and the more commonly observed broadband gamma activity. The power of narrow and broadband gamma activity were uncorrelated, and visual contrast suppressed narrowband gamma while it increased broadband gamma. Within cortex, narrowband gamma was strongest in L4, and intracellular recordings in cortex revealed that narrowband gamma was observed in excitatory, but

not inhibitory synaptic currents. Narrowband gamma oscillations persisted in LGN ensembles and L4 synaptic inputs, even after silencing of cortex.

We therefore conclude that the narrowband gamma oscillation represents an entirely different phenomenon than broadband gamma, one that is generated before the cortex: in thalamus and possibly even in retina. Whereas broadband gamma strongly involves cortical inhibitory networks (Cardin et al.,2009; Penttonen et al.,1998; Sohal et al.,2009; Wang and Buzsaki,1996), narrowband gamma is transmitted to cortex by the rhythmic firing of thalamic ensembles. Although resonance in thalamocortical loops has been proposed as a mechanism for the generation of high-frequency oscillations (Steriade,1997, 2000), we found that narrowband gamma was transmitted from LGN to visual cortex even after cortical firing was abolished optogenetically. We therefore propose that the oscillation is generated either within thalamic circuits, or by their interactions with their retinal inputs.

Our results are consistent with previous reports of narrowband oscillations in mouse visual cortex at frequencies close to 60 Hz (Lee et al.,2014; Niell and Stryker,2010). Furthermore, the oscillation we study here might be homologous to an oscillation previously described in LGN of anesthetized cats (Castelo-Branco et al.,1998; Koepsell et al.,2010; Neuenschwander and Singer,1996), which showed extremely narrowband rhythmicity within single recordings, although the frequency of this oscillation varied between recordings, spanning a range of 45 to 114 Hz. In these cat recordings, the thalamic oscillation was highly synchronous with a retinal oscillation determined either by simultaneous recording, or by analysis of intracellular EPSPs in thalamus. If this proposed homology is correct, it would suggest that the narrowband gamma recorded here might reflect an oscillation generated in retina and transmitted through LGN to visual cortex. The fact that the power of this oscillation can be altered by locomotion suggests that if the oscillation is indeed retinally-generated, its amplitude reflects locomotion-dependent filtering by thalamic circuitry, unless there exists some as-yet undetermined effect of locomotion on retinal physiology.

What function might this narrowband gamma oscillation play in visual processing? Although a definitive answer to this question requires further work, the present data are sufficient to formulate two hypotheses.

A first hypothesis is that the narrow band gamma oscillation represents an “idling” rhythm. In this interpretation, narrowband gamma represents a default state of LGN activity when visual processing is not being carried out, similar to the proposed function of the visual alpha rhythm and the beta oscillation of the motor system. This hypothesis would explain why this oscillation is suppressed by sudden increases in visual contrast.

In the second hypothesis, the narrow and broadband gamma oscillations would represent specific channels for thalamocortical and corticocortical communication. It has been proposed that oscillatory patterns with different frequency characteristics may allow routing of information between specific brain structures. For example, the coherence of slow gamma between hippocampal areas CA1 and CA3, and fast gamma between CA1 and entorhinal cortex (Colgin et al.,2009), may indicate the existence of two separate transmission channels in the hippocampal formation. Analogously, the narrowband gamma oscillation may provide a specific channel for feedforward transmission from LGN to visual cortex, whereas broadband gamma – which is

generated in multiple cortical regions – instead reflects the transmission of information within and between cortical circuits.

Acknowledgements

ABS, MC and KDH are funded by the Wellcome Trust (grant 095668 and 095669) and by the Simons Collaboration in the Global Brain (grant 325512). KDH is also funded by the EPSRC (K015141). MC holds the GlaxoSmithKilne/Fight for Sight Chair in Visual Neuroscience. MRR and LB were supported by funds awarded to the Centre for Integrative Neuroscience (DFG EXC 307). ADL and KR performed the experiments in Massimo Scanziani's lab with the support of the Howard Hughes Medical Institute and the Gatsby Charitable Foundation. KR was also supported by the National Science Foundation Graduate Research Program Fellowship.

Figures

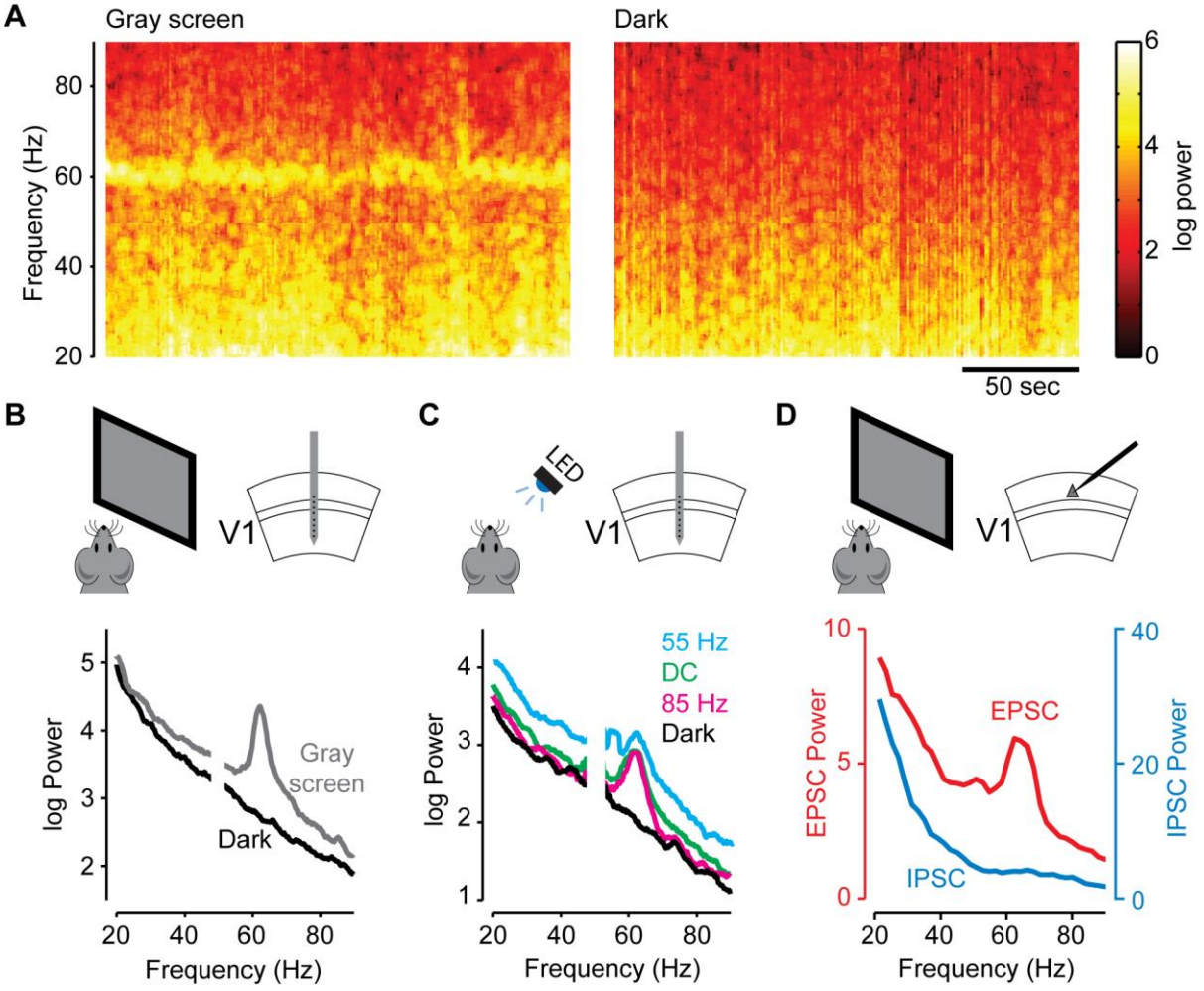

Figure 1: Narrowband gamma in mouse visual cortex. A. Spectrogram showing the variation of local field potential (LFP) power at frequencies 20-90 Hz with time. The LFP was recorded in the primary visual cortex (V1) of mice running on a treadmill during uniform gray (left) or complete darkness (right). **B.** The average power of the LFP as a function of frequency during uniform gray screen conditions (gray) or complete darkness (black) (same recording shown in **A**). **C.** Power of the LFP as a function of frequency under various conditions of LED stimulation: flickering at 55 Hz (cyan), 85 Hz (magenta), constantly on (DC, green), and off (Dark, black). **D.** Power in the excitatory post-synaptic

currents (EPSCs, red; whole-cell voltage-clamp recording at -70 mV) and inhibitory post-synaptic currents (IPSCs, blue; whole-cell voltage-clamp recording at +20 mV) in L2/3 neurons in V1, recorded during the uniform gray condition (Average spectra across 11 recorded neurons).

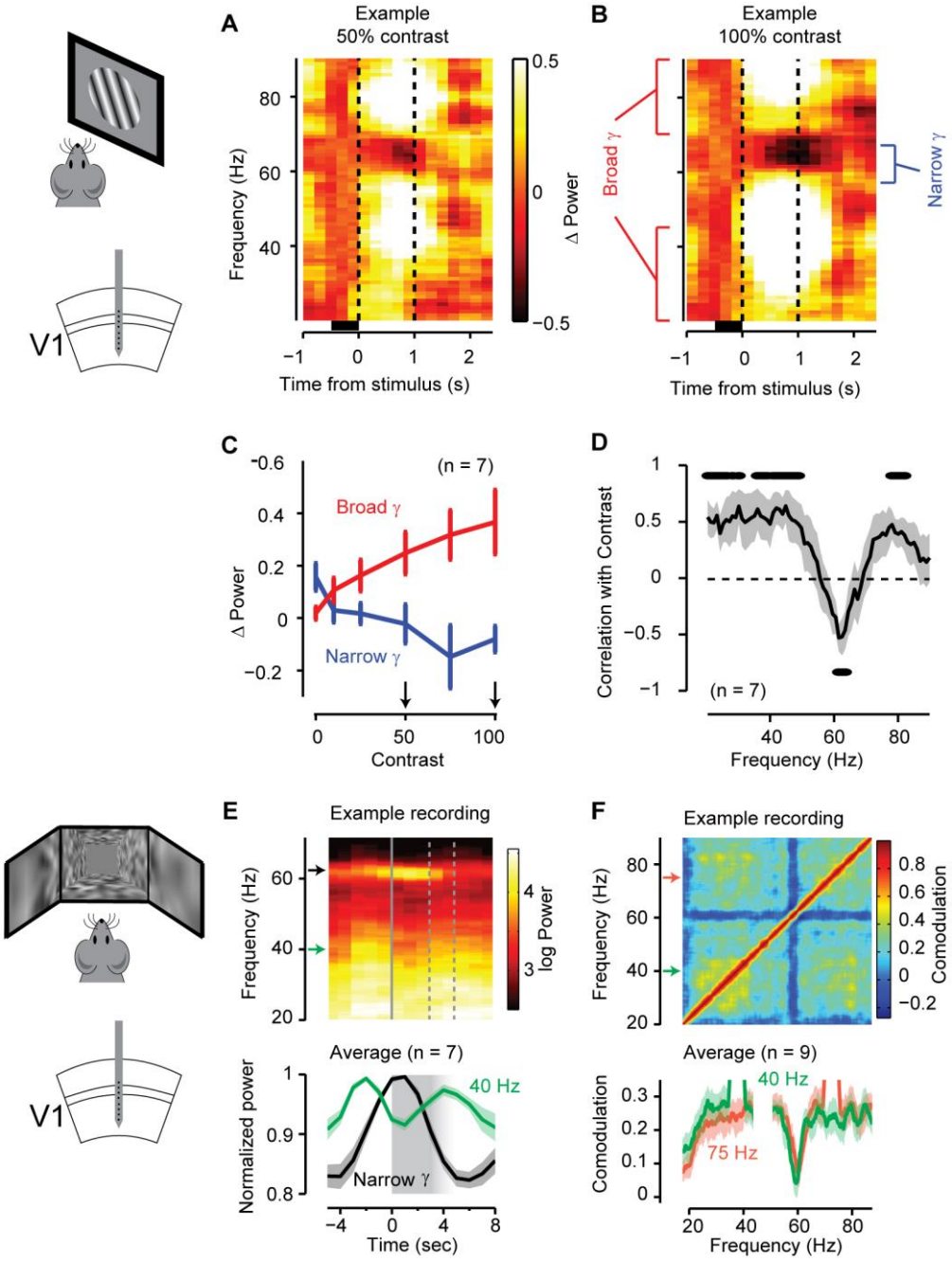

Figure 2: Narrowband gamma oscillations are suppressed by visual contrast. A-B. Average LFP spectrogram triggered on presentation of a drifting grating stimulus at 50% contrast (**A**) and 100% contrast (**B**), in a single experiment. The average baseline power at each frequency (0.5s before the stimulus onset, black bar) is subtracted before averaging across multiple repeats (20 repeats) of the same stimulus. Dotted lines indicate the period of presentation of a 50° sinusoidal drifting grating, in

the retinotopic location of the recorded area. **C.** Variation in power at the end of the stimulus presentation period (1 sec) as a function of visual contrast for narrowband gamma (Blue) and broadband gamma (Red). Narrowband gamma was calculated as the mean across the 55-65 Hz band; broadband gamma was calculated as the mean across bands 20-40 and 70-90 Hz and at stimulus offset (indicated in **B**). **D.** The correlation of the power at different frequencies with contrast. The shaded area shows the mean ± s.e.m. The dots above show the frequencies which had a significant positive correlation with contrast, while the dots below show frequencies with a significant negative correlation ($p<0.05$, $n = 7$). **E.** The power across frequencies triggered on the onset of the gray screen period in a virtual reality environment. The gray screen period lasted between 3-5 secs after which the animal re-enters the high contrast virtual environment. **(Bottom)** normalized power (power / maximal power) at the narrow band frequency (Narrowband gamma; black) and at 40Hz (Green). The shaded region shows the mean ± s.e.m across 7 recording sessions. **F.** The co-modulation of the power at different frequencies; i.e. the correlation in the power of different frequency bands, in an example recording. The blue cross visible at 60 Hz indicates that narrowband gamma power is uncorrelated with broadband gamma power. **(Bottom)** The co-modulation of 40 Hz (green) and 75 Hz (red) with respect to other frequency bands, showing a dip at the narrowband gamma frequency. The shaded area shows the mean ± s.e.m across 10 recordings in a virtual reality environment. The arrows in **E** and **F** indicate the frequencies shown in the bottom plots.

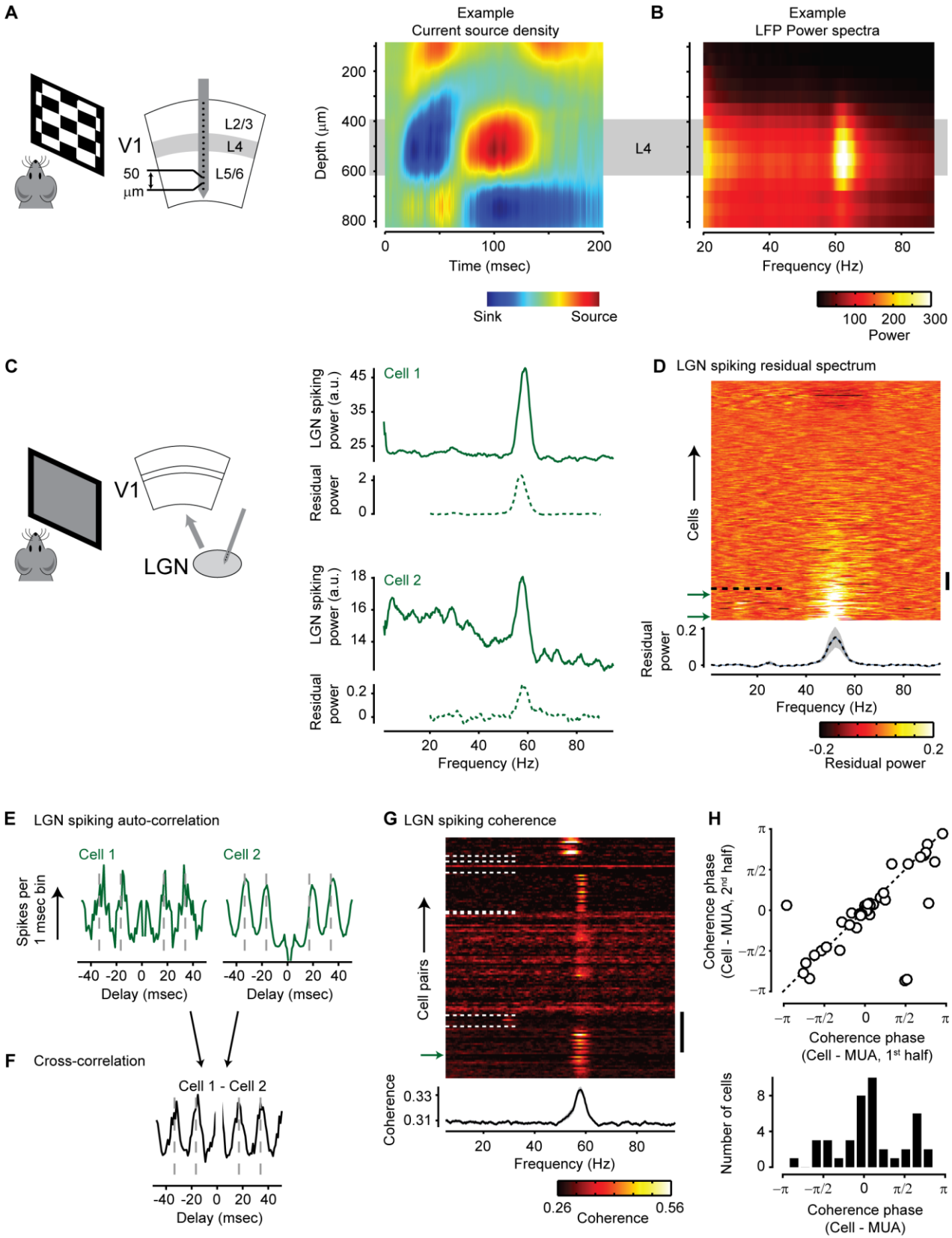

Figure 3: Narrowband gamma is highest in Layer 4 of V1 and present in LGN spiking activity. A. We recorded across the laminae of primary visual cortex using a 16-channel multi-electrode array. Example current source density analysis across the laminar probe that shows that layer 4, identified

as the location of the earliest current sink in response to a checkerboard stimulus, was present between 400-600 µm along the electrode. **B.** Mean spectral power at different frequencies, calculated at different cortical depths (same recording as **A**), showing highest narrowband gamma power close to Layer 4. **C.** Extracellular recordings from the LGN using a multi-electrode array in vivo. The spiking power spectra show a clear gamma modulation (two example neurons). Below each spectrum, the dotted line shows the fractional increase in power from a fit on the spectra (residual power spectrum). **D.** Pseudocolor plot showing residual spectra of all recorded LGN neurons (n = 323), ordered by gamma power. The mean ± s.e.m of the residual power across the population is shown at the bottom. Cells with residual gamma power over 0.20 are below the black dotted line (44 cells). The vertical scale bar indicates 20 cells, and the green arrows point to the examples shown in panels C, E & F. **E.** Two examples of the spike auto-correlation of LGN neurons (same cells as C), showing a clear oscillation at narrowband gamma frequency. Dashed lines indicate the positions of the peaks expected for a 60 Hz modulation (at ±16.7 and ±33.4 msec). **F.** The cross-correlation of spike times of neurons in G. **G.** The coherence spectra of cell pairs of simultaneously recorded neurons with residual gamma power greater than 0.20 (n = 130 cell pairs). White dotted lines separate pairs from different recording sessions. The mean ± s.e.m of the coherence spectra across all cell pairs is shown at the bottom. The scale bar indicates 20 cell pairs, and the green arrow points to the example cell pair shown in in panels F. **H.** (Top) Phase of coherence of the narrowband frequency between a cell and the population of other simultaneously recorded cells calculated in the first and second halves of the recording. (Bottom) The distribution of the coherence phase angles across cells (n = 44 cells).

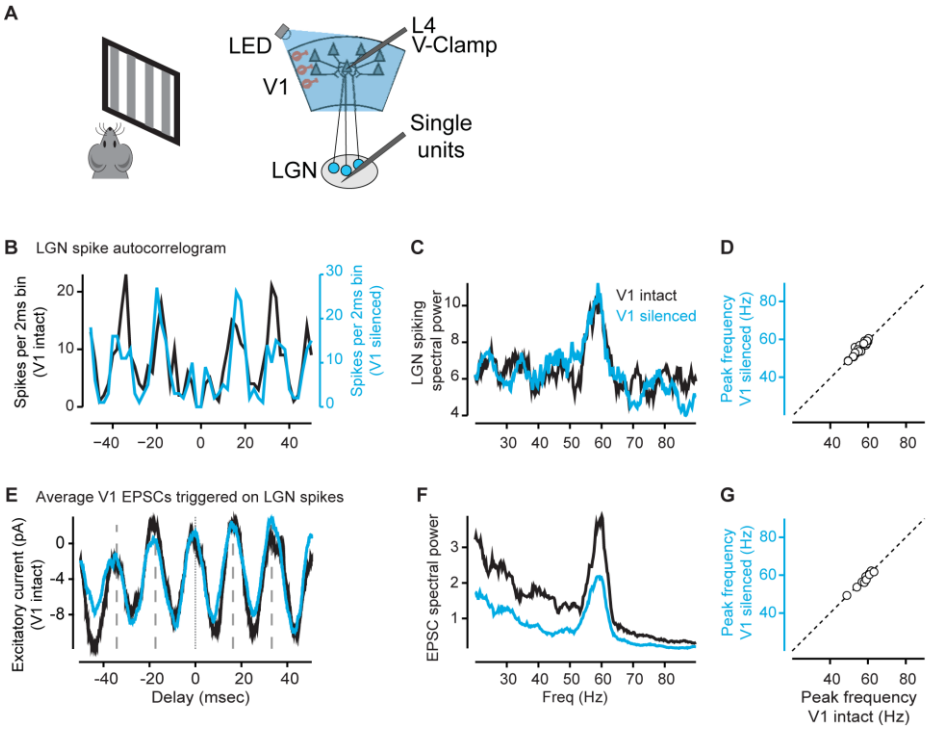

Figure 4: Narrowband gamma oscillations in LGN are independent of V1 activity. A. We made whole-cell voltage-clamp recordings of EPSCs in neurons in layer 4 of V1 (under urethane anaesthesia), while simultaneously recording single-unit activity in the LGN. V1 could be silenced by shining a blue LED over the region. **B.** Spike time autocorrelation of a LGN single unit when V1 activity was intact (black) or silenced (cyan). **C.** Spectral power of the same neuron in the two

conditions, showing that the presence and frequency of the peak in narrow-band power remains unaffected by cortical silencing. **D.** Comparison of the peak frequency of the narrow-band gamma when cortical activity is intact or silenced (n = 14 recordings). **E.** Average EPSCs recorded by voltage-clamping a V1 layer 4 neuron at -70mV, triggered on spikes of an LGN neuron (same neuron as in B, C), when V1 activity was intact (black) or silenced (cyan). Excitatory current negative. **F.** The spectral power of EPSCs in the same neurons. **G.** Comparison of the peak-frequency of the narrow-band gamma when the cortical activity is intact or silenced.

References

Ayaz, A., Saleem, A.B., Scholvinck, M.L., and Carandini, M. (2013). Locomotion controls spatial integration in mouse visual cortex. Curr Biol 23, 890-894.

Bragin, A., Jando, G., Nadasdy, Z., Hetke, J., Wise, K., and Buzsaki, G. (1995). Gamma (40-100 Hz) oscillation in the hippocampus of the behaving rat. J Neurosci 15, 47-60.

Cardin, J.A., Carlen, M., Meletis, K., Knoblich, U., Zhang, F., Deisseroth, K., Tsai, L.H., and Moore, C.I. (2009). Driving fast-spiking cells induces gamma rhythm and controls sensory responses. Nature 459, 663-667.

Castelo-Branco, M., Neuenschwander, S., and Singer, W. (1998). Synchronization of visual responses between the cortex, lateral geniculate nucleus, and retina in the anesthetized cat. J Neurosci 18, 6395-6410.

Chalk, M., Herrero, J.L., Gieselmann, M.A., Delicato, L.S., Gotthardt, S., and Thiele, A. (2010). Attention reduces stimulus-driven gamma frequency oscillations and spike field coherence in V1. Neuron 66, 114-125.

Colgin, L.L., Denninger, T., Fyhn, M., Hafting, T., Bonnevie, T., Jensen, O., Moser, M.B., and Moser, E.I. (2009). Frequency of gamma oscillations routes flow of information in the hippocampus. Nature 462, 353-357.

Eckhorn, R., Bauer, R., Jordan, W., Brosch, M., Kruse, W., Munk, M., and Reitboeck, H.J. (1988). Coherent oscillations: a mechanism of feature linking in the visual cortex? Multiple electrode and correlation analyses in the cat. Biol Cybern 60, 121-130.

Engel, A.K., Fries, P., and Singer, W. (2001). Dynamic predictions: oscillations and synchrony in top-down processing. Nature reviews Neuroscience 2, 704-716.

Erisken, S., Vaiceliunaite, A., Jurjut, O., Fiorini, M., Katzner, S., and Busse, L. (2014). Effects of locomotion extend throughout the mouse early visual system. Curr Biol 24, 2899-2907.

Fries, P. (2005). A mechanism for cognitive dynamics: neuronal communication through neuronal coherence. Trends in cognitive sciences 9, 474-480.

Fries, P. (2009). Neuronal gamma-band synchronization as a fundamental process in cortical computation. Annu Rev Neurosci 32, 209-224.

Fries, P., Reynolds, J.H., Rorie, A.E., and Desimone, R. (2001). Modulation of oscillatory neuronal synchronization by selective visual attention. Science 291, 1560-1563.

Gieselmann, M.A., and Thiele, A. (2008). Comparison of spatial integration and surround suppression characteristics in spiking activity and the local field potential in macaque V1. Eur J Neurosci 28, 447-459.

Gray, C.M., and Singer, W. (1989). Stimulus-specific neuronal oscillations in orientation columns of cat visual cortex. Proc Natl Acad Sci U S A 86, 1698-1702.

Haider, B., Hausser, M., and Carandini, M. (2013). Inhibition dominates sensory responses in the awake cortex. Nature 493, 97-100.

Hasenstaub, A., Shu, Y., Haider, B., Kraushaar, U., Duque, A., and McCormick, D.A. (2005). Inhibitory postsynaptic potentials carry synchronized frequency information in active cortical networks. Neuron 47, 423-435.

Koepsell, K., Wang, X., Hirsch, J.A., and Sommer, F.T. (2010). Exploring the function of neural oscillations in early sensory systems. Frontiers in neuroscience 4, 53.
Kreiter, A.K., and Singer, W. (1992). Oscillatory Neuronal Responses in the Visual-Cortex of the Awake Macaque Monkey. European Journal of Neuroscience 4, 369-375.
Lee, A.M., Hoy, J.L., Bonci, A., Wilbrecht, L., Stryker, M.P., and Niell, C.M. (2014). Identification of a brainstem circuit regulating visual cortical state in parallel with locomotion. Neuron 83, 455-466.
Lien, A.D., and Scanziani, M. (2013). Tuned thalamic excitation is amplified by visual cortical circuits. Nat Neurosci 16, 1315-1323.
Lisman, J.E., and Idiart, M.A. (1995). Storage of 7 +/- 2 short-term memories in oscillatory subcycles. Science 267, 1512-1515.
McGinley, M.J., David, S.V., and McCormick, D.A. (2015a). Cortical Membrane Potential Signature of Optimal States for Sensory Signal Detection. Neuron 87, 179-192.
McGinley, M.J., Vinck, M., Reimer, J., Batista-Brito, R., Zagha, E., Cadwell, C.R., Tolias, A.S., Cardin, J.A., and McCormick, D.A. (2015b). Waking State: Rapid Variations Modulate Neural and Behavioral Responses. Neuron 87, 1143-1161.
Middleton, S.J., Racca, C., Cunningham, M.O., Traub, R.D., Monyer, H., Knopfel, T., Schofield, I.S., Jenkins, A., and Whittington, M.A. (2008). High-frequency network oscillations in cerebellar cortex. Neuron 58, 763-774.
Mitzdorf, U. (1985). Current source-density method and application in cat cerebral cortex: investigation of evoked potentials and EEG phenomena. Physiol Rev 65, 37-100.
Neuenschwander, S., and Singer, W. (1996). Long-range synchronization of oscillatory light responses in the cat retina and lateral geniculate nucleus. Nature 379, 728-732.
Niell, C.M., and Stryker, M.P. (2010). Modulation of visual responses by behavioral state in mouse visual cortex. Neuron 65, 472-479.
Penttonen, M., Kamondi, A., Acsady, L., and Buzsaki, G. (1998). Gamma frequency oscillation in the hippocampus of the rat: intracellular analysis in vivo. Eur J Neurosci 10, 718-728.
Pesaran, B., Pezaris, J.S., Sahani, M., Mitra, P.P., and Andersen, R.A. (2002). Temporal structure in neuronal activity during working memory in macaque parietal cortex. Nat Neurosci 5, 805-811.
Popescu, A.T., Popa, D., and Pare, D. (2009). Coherent gamma oscillations couple the amygdala and striatum during learning. Nat Neurosci 12, 801-807.
Reimer, J., Froudarakis, E., Cadwell, C.R., Yatsenko, D., Denfield, G.H., and Tolias, A.S. (2014). Pupil fluctuations track fast switching of cortical states during quiet wakefulness. Neuron 84, 355-362.
Reinhold, K., Lien, A.D., and Scanziani, M. (2015). Distinct recurrent versus afferent dynamics in cortical visual processing. Nat Neurosci 18, 1789-1797.
Saleem, A.B., Ayaz, A., Jeffery, K.J., Harris, K.D., and Carandini, M. (2013). Integration of visual motion and locomotion in mouse visual cortex. Nat Neurosci 16, 1864-1869.
Singer, W. (1999). Neuronal synchrony: a versatile code for the definition of relations? Neuron 24, 49-65, 111-125.
Sohal, V.S., Zhang, F., Yizhar, O., and Deisseroth, K. (2009). Parvalbumin neurons and gamma rhythms enhance cortical circuit performance. Nature 459, 698-702.
Steriade, M. (1997). Synchronized activities of coupled oscillators in the cerebral cortex and thalamus at different levels of vigilance. Cereb Cortex 7, 583-604.
Steriade, M. (2000). Corticothalamic resonance, states of vigilance and mentation. Neuroscience 101, 243-276.
Tallon, C., Bertrand, O., Bouchet, P., and Pernier, J. (1995). Gamma-range activity evoked by coherent visual stimuli in humans. Eur J Neurosci 7, 1285-1291.
Veit, J., Bhattacharyya, A., Kretz, R., and Rainer, G. (2011). Neural response dynamics of spiking and local field potential activity depend on CRT monitor refresh rate in the tree shrew primary visual cortex. J Neurophysiol 106, 2303-2313.
Vinck, M., Batista-Brito, R., Knoblich, U., and Cardin, J.A. (2015). Arousal and locomotion make distinct contributions to cortical activity patterns and visual encoding. Neuron 86, 740-754.

Wang, X.J., and Buzsaki, G. (1996). Gamma oscillation by synaptic inhibition in a hippocampal interneuronal network model. J Neurosci 16, 6402-6413.

Williams, P.E., Mechler, F., Gordon, J., Shapley, R., and Hawken, M.J. (2004). Entrainment to video displays in primary visual cortex of macaque and humans. J Neurosci 24, 8278-8288.